DOKUZ EYLÜL UNIVERSITY

GRADUATE SCHOOL OF NATURAL AND APPLIED SCIENCES

DYNAMIC ANALYSIS OF COMPOSITE LAMINATED PLATES

by

Turan ERÇOPUR

September, 2010

İZMİR

DYNAMIC ANALYSIS OF COMPOSITE LAMINATED PLATES

A Thesis Submitted to the
Graduate School of Natural and Applied Sciences of Dokuz Eylül University
In Partial Fulfillment of the Requirements for the Degree of Master of Science
in Mechanical Engineering, Mechanics Program

by
Turan ERÇOPUR

September, 2010
İZMİR

M.Sc THESIS EXAMINATION RESULT FORM

We have read the thesis entitled **"DYNAMIC ANALYSIS OF COMPOSITE LAMINATED PLATES"** completed by **TURAN ERÇOPUR** under supervision of **ASSIST. PROF. BİNNUR GÖREN KIRAL** and we certify that in our opinion it is fully adequate, in scope and in quality, as a thesis for the degree of Master of Science.

.....

Assist. Prof. Binnur GÖREN KIRAL

Supervisor

.....	.....
Prof. Dr. Seçil ERİM	Assoc. Prof. Dr. Mustafa TOPARLI
(Jury Member)	(Jury Member)

Prof.Dr. Mustafa SABUNCU
Director
Graduate School of Natural and Applied Sciences

ACKNOWLEDGMENTS

I would like to express my deepest gratitude and thanks to my supervisor Assist. Prof. Dr. Binnur GÖREN KIRAL for her continuous support, excellent guidance, and valuable advice throughout the progress of this thesis.

I would like to express my thanks to Assist. Prof. Dr. Zeki KIRAL for his assistance and guidance, and valuable advice throughout the experimental study of this thesis.

Finally, I am deeply indebted to my family and friends for their encouragement and continuous morale support.

Turan ERÇOPUR

DYNAMIC ANALYSIS OF COMPOSITE LAMINATED PLATES

ABSTRACT

This thesis reports the finite element analysis of dynamic responses of laminated composite plates, which are subjected to delamination. Parametric input files are developed by using ANSYS software in order to determine the natural frequencies and associated mode shapes with the harmonic responses of the laminated composite plates. Effects of delamination width and location on the natural frequency of both clamped-free and clamped-pinned laminated composite plates and harmonic response of a clamped-free laminated composite plate, which have a circular strip delamination around a circular hole delamination, are investigated. Comparisons with the results in literature verify the validity of the present study. As a result, it is seen that the natural frequency decreases in the existence of the delamination and the decreasing level depends on the width and location of the delamination.

Keywords: Composite plate, delamination, natural frequency, dynamic response

TABAKALI KOMPOZİT PLAKALARIN DİNAMİK ANALİZİ

ÖZ

Bu tez, delaminasyona uğramış tabakalı kompozit plakaların dinamik cevaplarının sonlu eleman analizlerini ortaya koymaktadır. Tabakalı kompozit plakaların harmonik yanıtları ile birlikte doğal frekanslarını ve ilgili mod şekillerini hesaplamak için ANSYS yazılımı kullanılarak parametrik girdi dosyaları geliştirilmiştir. Ankastre-serbest ve ankastre-kayar mesnetli tabakalı kompozit plakalarda delaminasyon genişliğinin ve konumunun doğal frekansa etkisi ve dairesel boşluk etrafında dairesel şerit delaminasyonuna sahip ankastre-serbest mesnetli tabakalı bir kompozit plakanın harmonik yanıtı incelenmiştir. Literatürdeki sonuçlarla yapılan karşılaştırmalar bu çalışmanın geçerliliğini doğrulamaktadır. Sonuç olarak, delaminasyon varlığında doğal frekansın azaldığı ve azalma derecesinin delaminasyon genişliğine ve konumuna bağlı olduğu görülmüştür.

Anahtar sözcükler: Kompozit plaka, delaminasyon, doğal frekans, dinamik cevap

CONTENTS

Page

CHAPTER ONE

INTRODUCTION

Along with the progress of industry, the quality of engineering of the structural materials has continued to improve while their harms have continued to decrease. Cause of their high stiffness and strength to low weight, the use of composite materials especially in automotive, construction and aerospace industries and various machine components has been increasing considerably in the last decades.

However, the mechanical properties of composite materials may degrade severely in the presence of damage. It is well known that delamination is one of the most important failure modes of composite materials. Manufacturing defects such as air entrapment or insufficient resin during fabrication, external impacts, or compression loads may cause delamination in composite plates. These delaminations and their further extensions lead to loss of stiffness and strength of the composite materials. Decreasing of the stiffness also affects the vibration characteristics of the structure. This decreasing level depends on the size, location, and shape of the delamination in the composite materials. In the design stage, it is very important to determine the natural frequencies since the resonance phenomena occurs when the operating frequency is close to one of the natural frequencies of the structure.(Gören Kıral, 2009)

Dynamic behaviors of the laminated composite structures have been investigated by many researchers with analytical, numerical, and experimental methods according to the type of the problem. Most of the publications of dynamic behaviors of laminated composite structures are based on the classical laminated plate theory. In this theory, the transverse shear deformation effect is ignored. Qatu (1991) published results for the natural frequencies of laminated composite plates having rectangular shapes under different boundary conditions. Qatu (1994) published also results for the natural frequencies of laminated plates having triangular and trapezoidal shape.

However, it is difficult to obtain exact analytical solutions for the multilayered composites having arbitrary lamination sequence with different boundary conditions. This difficulty increases considerably in the presence of delamination. As a result, computational approaches, e.g. finite element method, are used to obtain the exact solutions for these problems.

Sankar (1991) modeled a delaminated beam as two sublaminates by offset finite element method. Rikards (1993) developed a finite superelement model for composite beams and plates, each layer being considered as a simple Timoshenko beam. Gadelrab (1996) discussed the effect of the delamination length and location on the natural frequencies of composite laminated beam under different boundary conditions using the finite element method. Zak et al. (2000), Ousset and Roudolff (2000) developed finite element models for beams and plates with boundary delamination. Lee (2000) developed a finite element model using a layer wise theory to formulate the free vibration analysis of a delaminated composite beam and found that the layer wise approach is adequate for vibration analysis of delaminated composite beams. Hua et al. (2002) investigated the effects of delamination on the vibration characteristic of composite laminated plates using a high-order finite element, which satisfies the zero transverse shear strain condition on the top and bottom surfaces of laminated plates. Yam et al. (2004) established a three-dimensional finite element model for multilayered composites with internal delamination, which virtual elements were adopted in the region of the delamination to prevent element penetration. Alnefaie (2009) calculated natural frequencies and modal displacements of rectangular delaminated composite plates and showed that the good agreement between the numerical results and available experimental data.

In this thesis, dynamic responses of laminated composite plates, which are subjected to delamination, are investigated. Parametric input files are developed by using ANSYS software in order to determine the natural frequencies and associated mode shapes with the harmonic responses of the laminated composite plates. There-dimensional finite element model of laminated composite plates are formed and the natural frequencies are determined. Good agreements are seen between the numerical

results and the available experimental data. In the light of this compatibility, the finite element models having different delamination width and location are formed and effects of delamination width and location on the natural frequency of both clamped-free and clamped-pinned laminated composite plates are determined. In addition to these, harmonic response of a clamped-free laminated composite plate, which has a circular strip delamination around a circular hole delamination, are investigated.

CHAPTER TWO

LAMINATED COMPOSITE MATERIALS

2.1 Introduction to Laminated Composite Materials

Laminated composite materials consist of layers of at least two different materials that are bonded together. Lamination is used to combine best aspects of the constituent layers and bonding material in order to achieve a more useful material. The properties that can be emphasized by lamination are strength, stiffness, low weight, corrosion resistance, wear resistance, thermal insulation, acoustical insulation, etc. (Jones, 1975)

Commonly accepted types of laminated composite materials are bimetals, clad metals, laminated glass, plastic-based laminates, and laminated fiber-reinforced composite materials. These types of laminated composite materials are described and discussed in the following subsections.

2.2 Bimetals

Bimetals are laminates of two different metals that usually have significantly different coefficients of thermal expansion. Under change in temperature, bimetals warp or deflect a predictable amount and are therefore well suited for use in temperature-measuring devices. For example, a simple thermostat can be made from a cantilever strip of two metals having different coefficients of thermal expansion bonded together.

2.3 Clad Metals

The cladding of one metal with another is done to obtain the best properties of both. For example, high-strength aluminum alloys do not resist corrosion; however, some aluminum alloys are very corrosion resistant. Thus, a high-strength aluminum

alloy covered with a corrosion-resistant aluminum alloy is a composite material with both high strength and the corrosion resistant.

2.4 Laminated Glass

The concept of protection of one layer of material by another as described in the previous subsection has been extended in a rather unique way to safety glass, which is a layer of polyvinyl butyral sandwiched between two layers of glass. The glass protects the plastic from scratching and gives it stiffness. The plastic provides the toughness to the glass. Thus, together, the glass and plastic protect each other in different ways and lead to a composite material with properties that are vastly improved over those of its constituents. In fact, the high-scretchability property of the plastic is eliminated because it is the inner layer.

2.5 Plastic Based Laminates

Many materials can be saturated with various plastics for a variety of purposes. Formica is a good example of compound composite materials. It is merely layers of heavy kraft paper impregnated with a phenolic resin overlaid by a plastic-saturated decorative sheet, which is overlaid with a plastic-saturated cellulose mat. Heat and pressure are used to bond the layers together. A useful variation on theme is obtained when an aluminum layer is placed between the decorative layer and kraft paper layer to dissipate quickly the heat of, for example, a burning cigarette or hot pan on a kitchen counter instead of leaving a burned spot.

2.6 Laminated Fiber-Reinforced Composite Materials

Layers of fiber-reinforced material are built up with the fiber directions of each layer typically oriented in different directions to give different strengths and stiffness in the various directions. Thus, the strength and stiffness of the laminated fiber-

reinforced composite can be tailored to the specific design requirements of the structural element being built.

The basic building block of a laminate is a lamina which is a flat (sometimes curved as in a shell) arrangement of unidirectional fibers or woven fibers in a matrix. Two typical flat laminas along with their principal material axes, which are parallel and perpendicular to the fiber directional, are shown in Figure 2.1. The fibers are the principal reinforcing or load-carrying agent and are typically strong and stiff. The matrix can be organic, metallic, ceramic, or carbon. The function of the matrix is to support and protect the fibers and provide a means of distributing load among, and transmitting load between, the fibers.

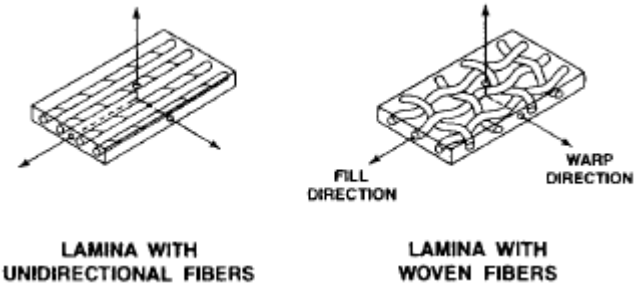

Figure 2.1 Two principal types of laminae (Jones, 1975)

A laminate is a bonded stack of lamina with various orientations of principal material directions in the laminae. The layers of a laminate are usually bonded together by the same matrix material that is used in the individual lamina. Laminates can be composed of the plates of different materials or layers of fiber-reinforced laminae.

A major purpose of lamination is to tailor the directional dependence of strength and stiffness of a composite material to match the loading environment of the structural element. Laminates are uniquely suited to this objective because the principal material directions of each layer can be oriented according to need.

CHAPTER THREE

DELAMINATION IN COMPOSITE MATERIALS

3.1 Introduction to Delamination in Composite Materials

The use of composite materials, especially in the form of fiber reinforced laminated, has been increasing in the design of various structural applications. This is mostly caused these materials having a higher strength to weight ratio than the ordinary engineering of the structural materials. In spite of their advantages, the mechanical properties of composite materials may degrade severely in the presence of damage. It is well known that delamination is one of the most important failure modes of composite materials.

Manufacturing defects such as air entrapment or insufficient resin during fabrication, external impacts, or compression loads may cause delamination in composite plates. These delaminations and their further extensions lead to loss of stiffness and the strength of the composite materials. Decreasing of the stiffness also affects the vibration characteristics of the structure. In addition, in the presence of the delamination, buckling load of the material decreases. Therefore, that composite material buckles at lower and delamination area growths when the composite material is subjected to a compressive load.

3.2 Causes of Delamination in Composite Materials

Commonly accepted causes of delamination in laminated composite materials are manufacturing defects, external impacts, and interlaminar stresses. These causes are described and discussed in the following paragraphs.

Manufacturing defects such as air entrapments, impurities, improper techniques, and insufficient resin during the fabrication can result a separation between the layers of laminated composites.

High velocity impact causes a significant surface damage, so that it should be easily recognized. The area of surface damage increases linearly with the component thickness. In addition to the surface damage, it may cause a significant delamination around the impact location.

Low velocity impact causes internal delamination. In presence of this damage, it is not possible to see a significant sign on the surfaces of the materials. Therefore, that internal delaminations and loss of the structural integrity may remain undetected.

Laminated composite materials can exhibit high directional strength properties. This advantage enables to designers to align purposely the plies in the direction of load. However, when the direction of the load is out of the plies or the load is transferred to adjacent plies, interlaminar stresses may cause delamination in the laminated composite material. Interlaminar stresses can also be introduced by compressive loading. This causes buckling of the plies and subsequently delamination in the composite material.

CHAPTER FOUR

THEORY OF ELASTICITY

4.1 Constitutive Equations in Local Coordinates

Assume that the individual lamina is orthotropic with fiber orientation along x_1 axis of the local material coordinate system x_1, x_2, x_3 as shown.

The strains in local material coordinates are define as

$$\varepsilon_1 = \frac{\partial u}{\partial x_1} \qquad \varepsilon_2 = \frac{\partial v}{\partial x_2} \qquad \varepsilon_3 = \frac{\partial w}{\partial x_3} \tag{4.1}$$

$$\gamma_{23} = \frac{\partial v}{\partial x_3} + \frac{\partial w}{\partial x_2} \qquad \gamma_{31} = \frac{\partial w}{\partial x_1} + \frac{\partial u}{\partial x_3} \qquad \gamma_{12} = \frac{\partial u}{\partial x_2} + \frac{\partial v}{\partial x_1} \tag{4.2}$$

where u, v, w are displacements in the x_1, x_2, x_3 directions, respectively.

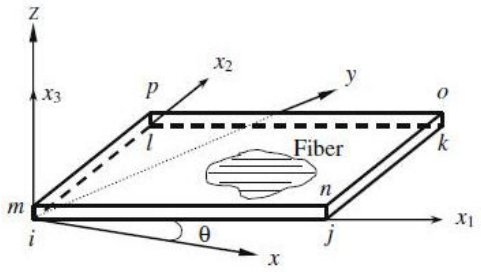

Figure 4.1 Composite plate (Alnefai, 2009)

The generalized Hooke's law as referred to the local coordinate system can be written as

$$\varepsilon_1 = \frac{1}{E_1}\sigma_1 - \frac{\nu_{21}}{E_2}\sigma_2 - \frac{\nu_{31}}{E_3}\sigma_3 \qquad \gamma_{23} = \frac{1}{G_{23}}\tau_{23} \tag{4.3}$$

$$\varepsilon_2 = \frac{1}{E_2}\sigma_2 - \frac{\nu_{12}}{E_1}\sigma_1 - \frac{\nu_{32}}{E_3}\sigma_3 \qquad \gamma_{31} = \frac{1}{G_{31}}\tau_{31} \tag{4.4}$$

$$\varepsilon_3 = \frac{1}{E_3}\sigma_3 - \frac{\nu_{13}}{E_1}\sigma_1 - \frac{\nu_{23}}{E_2}\sigma_2 \qquad \gamma_{12} = \frac{1}{G_{12}}\tau_{12} \tag{4.5}$$

where E_1, E_2, and E_3 are the elasticity modules along the principal material axes; ν_{12} is the poisson ratio that characterizes the decrease in the x_2 direction during the

tension applied in the x_1 direction; ν_{21} is the poisson ratio that characterizes the decrease in the x_1 direction during the tension applied in the x_2 direction, and so on; and G_{23}, G_{31}, and G_{12} are the shear modules that characterize the changes of angles between the principal direction x_2, x_3, x_1 and x_3, x_1 , x_2, respectively. Due to the symmetry, the following relations obtain:

$$E_1\nu_{21} = E_2\nu_{12} \qquad E_2\nu_{32} = E_3\nu_{23} \qquad E_3\nu_{13} = E_1\nu_{31} \tag{4.6}$$

The strain-stress relations in local material coordinates for an orthotropic lamina are

$$\begin{Bmatrix} \varepsilon_1 \\ \varepsilon_2 \\ \varepsilon_3 \\ \gamma_{23} \\ \gamma_{31} \\ \gamma_{12} \end{Bmatrix} = \begin{bmatrix} S_{11} & S_{12} & S_{13} & 0 & 0 & 0 \\ S_{12} & S_{22} & S_{23} & 0 & 0 & 0 \\ S_{13} & S_{23} & S_{33} & 0 & 0 & 0 \\ 0 & 0 & 0 & S_{44} & 0 & 0 \\ 0 & 0 & 0 & 0 & S_{55} & 0 \\ 0 & 0 & 0 & 0 & 0 & S_{66} \end{bmatrix} \begin{Bmatrix} \sigma_1 \\ \sigma_2 \\ \sigma_3 \\ \tau_{23} \\ \tau_{31} \\ \tau_{12} \end{Bmatrix} \tag{4.7}$$

where, the terms S_{11}, S_{22}, and S_{33} each represent extensional response to an individual applied stress σ_1, σ_2, and σ_3, respectively in the same direction. The terms S_{44}, S_{55}, and S_{66} represent shear strain response to an applied shear stress in the same plane. The terms S_{12}, S_{13}, and S_{23} represent coupling between dissimilar normal stresses and normal strains (extension-extension coupling more commonly known as the poisson effect). Note that there is no interaction between normal stresses and shear strains. Similarly, there is no interaction between shear stresses and shear strains in different planes. The terms of the compliance matrix are

$$S_{11} = \frac{1}{E_1} \qquad S_{12} = \frac{-\nu_{12}}{E_1} \qquad S_{13} = \frac{-\nu_{13}}{E_1}$$

$$S_{22} = \frac{1}{E_2} \qquad S_{23} = \frac{-\nu_{23}}{E_2}$$

$$S_{33} = \frac{1}{E_3}$$

$$S_{44} = \frac{1}{G_{23}} \qquad S_{55} = \frac{1}{G_{31}} \qquad S_{66} = \frac{1}{G_{12}}$$

The stress-strain relations in local material coordinates for an orthotropic lamina are

$$\begin{Bmatrix} \sigma_1 \\ \sigma_2 \\ \sigma_3 \\ \tau_{23} \\ \tau_{31} \\ \tau_{12} \end{Bmatrix} = \begin{bmatrix} C_{11} & C_{12} & C_{13} & 0 & 0 & 0 \\ C_{12} & C_{22} & C_{23} & 0 & 0 & 0 \\ C_{13} & C_{23} & C_{33} & 0 & 0 & 0 \\ 0 & 0 & 0 & C_{44} & 0 & 0 \\ 0 & 0 & 0 & 0 & C_{55} & 0 \\ 0 & 0 & 0 & 0 & 0 & C_{66} \end{bmatrix} \begin{Bmatrix} \varepsilon_1 \\ \varepsilon_2 \\ \varepsilon_3 \\ \gamma_{23} \\ \gamma_{31} \\ \gamma_{12} \end{Bmatrix} \tag{4.8}$$

Note that stiffness matrix is inverse of the compliance matrix. The terms of the stiffness matrix are

$$C_{11} = \frac{S_{22}S_{33} - S_{23}^2}{S} \qquad C_{12} = \frac{S_{13}S_{23} - S_{12}S_{33}}{S} \qquad C_{13} = \frac{S_{12}S_{23} - S_{13}S_{22}}{S}$$

$$C_{22} = \frac{S_{11}S_{33} - S_{13}^2}{S} \qquad C_{23} = \frac{S_{12}S_{13} - S_{11}S_{23}}{S}$$

$$C_{33} = \frac{S_{11}S_{22} - S_{12}^2}{S}$$

$$C_{44} = \frac{1}{S_{44}} \qquad C_{55} = \frac{1}{S_{55}} \qquad C_{66} = \frac{1}{S_{66}}$$

where

$$S = S_{11}S_{22}S_{33} - S_{11}S_{23}^2 - S_{22}S_{13}^2 - S_{33}S_{12}^2 + 2S_{12}S_{23}S_{13}$$

In summary, the constitutive equation in the local coordinate system for the lamina is

$$\{\sigma^*\} = [C]\{\varepsilon^*\} \tag{4.9}$$

where $\{\sigma^*\} = (\sigma_1, \sigma_2, \sigma_3, \tau_{23}, \tau_{31}, \tau_{12})^T$ and $\{\varepsilon^*\} = (\varepsilon_1, \varepsilon_2, \varepsilon_3, \gamma_{23}, \gamma_{31}, \gamma_{12})^T$ are vectors of stress and strain along the main directions in local coordinate system, respectively. $[C]$ is the stiffness matrix.

4.2 Constitutive Equations in Global Coordinates

The constitutive equation in the global coordinate system can be expressed as

$$\{\sigma\} = [A]\{\sigma^*\} = [A][C][A]^{-1}\{\varepsilon\} \tag{4.10}$$

where $\{\sigma\} = (\sigma_x, \sigma_y, \sigma_z, \tau_{yz}, \tau_{zx}, \tau_{xy})^T$ and $\{\varepsilon\} = (\varepsilon_x, \varepsilon_y, \varepsilon_z, \gamma_{yz}, \gamma_{zx}, \gamma_{xy})^T$ are vectors of stress and strain along the main directions in the global coordinate system, respectively. $[A]$ is transform matrix between the local and global coordinate system.

$$[A] = \begin{bmatrix} \cos^2\theta & \sin^2\theta & 0 & 0 & 0 & -2\sin\theta\cos\theta \\ \sin^2\theta & \cos^2\theta & 0 & 0 & 0 & 2\sin\theta\cos\theta \\ 0 & 0 & 1 & 0 & 0 & 0 \\ 0 & 0 & 0 & \cos\theta & \sin\theta & 0 \\ 0 & 0 & 0 & -\sin\theta & \cos\theta & 0 \\ \sin\theta\cos\theta & -\sin\theta\cos\theta & 0 & 0 & 0 & \cos^2\theta - \sin^2\theta \end{bmatrix}$$

The stress-strain relations in global coordinate system for an orthotropic lamina are

$$\begin{Bmatrix} \sigma_x \\ \sigma_y \\ \sigma_z \\ \tau_{yz} \\ \tau_{zx} \\ \tau_{xy} \end{Bmatrix} = \begin{bmatrix} \overline{C}_{11} & \overline{C}_{12} & \overline{C}_{13} & 0 & 0 & \overline{C}_{16} \\ \overline{C}_{12} & \overline{C}_{22} & \overline{C}_{23} & 0 & 0 & \overline{C}_{26} \\ \overline{C}_{13} & \overline{C}_{23} & \overline{C}_{33} & 0 & 0 & \overline{C}_{36} \\ 0 & 0 & 0 & \overline{C}_{44} & \overline{C}_{45} & 0 \\ 0 & 0 & 0 & \overline{C}_{45} & \overline{C}_{55} & 0 \\ \overline{C}_{16} & \overline{C}_{26} & \overline{C}_{36} & 0 & 0 & \overline{C}_{66} \end{bmatrix} \begin{Bmatrix} \varepsilon_x \\ \varepsilon_y \\ \varepsilon_z \\ \gamma_{yz} \\ \gamma_{zx} \\ \gamma_{xy} \end{Bmatrix} \tag{4.11}$$

The terms of the transformed stiffness matrix are

$$\overline{C}_{11} = C_{11}\cos^4\theta + 2(C_{12} + C_{66})\cos^2\theta\sin^2\theta + C_{22}\sin^4\theta$$

$$\overline{C}_{12} = C_{12}(\cos^4\theta + \sin^4\theta) + (C_{11} + C_{12} - 4C_{66})\cos^2\theta\sin^2\theta$$

$$\overline{C}_{13} = C_{13}\cos^2\theta + C_{23}\sin^2\theta$$

$$\overline{C}_{16} = (C_{11} - C_{12} - 2C_{66})\cos^3\theta\sin\theta + (C_{12} - C_{22} + 2C_{66})\cos\theta\sin^3\theta$$

$$\overline{C}_{22} = C_{22}\cos^4\theta + 2(C_{12} + 2C_{66})\cos^2\theta\sin^2\theta + C_{11}\sin^4\theta$$

$$\overline{C}_{23} = C_{23}\cos^2\theta + C_{13}\sin^2\theta$$

$$\overline{C}_{26} = (C_{12} - C_{22} + 2C_{66})\cos^3\theta\sin\theta + (C_{11} - C_{12} - 2C_{66})\cos\theta\sin^3\theta$$

$$\overline{C}_{33} = C_{33}$$

$$\overline{C}_{36} = (C_{13} - C_{23})\cos\theta\sin\theta$$

$$\overline{C}_{44} = C_{44}\cos^2\theta + C_{55}\sin^2\theta$$

$$\overline{C}_{45} = (C_{55} - C_{44})\cos\theta\sin\theta$$

$$\overline{C}_{55} = C_{55}\cos^2\theta + C_{44}\sin^2\theta$$

$$\overline{C}_{66} = (C_{11} + C_{22} - 2C_{12} - 2C_{66})\cos^2\theta\sin^2\theta + C_{66}(\cos^4\theta + \sin^4\theta)$$

The strain-stress relations in global coordinate system for an orthotropic lamina are

$$\begin{Bmatrix} \varepsilon_x \\ \varepsilon_y \\ \varepsilon_z \\ \gamma_{yz} \\ \gamma_{zx} \\ \gamma_{xy} \end{Bmatrix} = \begin{bmatrix} \overline{S}_{11} & \overline{S}_{12} & \overline{S}_{13} & 0 & 0 & \overline{S}_{16} \\ \overline{S}_{12} & \overline{S}_{22} & \overline{S}_{23} & 0 & 0 & \overline{S}_{26} \\ \overline{S}_{13} & \overline{S}_{23} & \overline{S}_{33} & 0 & 0 & \overline{S}_{36} \\ 0 & 0 & 0 & \overline{S}_{44} & \overline{S}_{45} & 0 \\ 0 & 0 & 0 & \overline{S}_{45} & \overline{S}_{55} & 0 \\ \overline{S}_{16} & \overline{S}_{26} & \overline{S}_{36} & 0 & 0 & \overline{S}_{66} \end{bmatrix} \begin{Bmatrix} \sigma_x \\ \sigma_y \\ \sigma_z \\ \tau_{yz} \\ \tau_{zx} \\ \tau_{xy} \end{Bmatrix} \tag{4.12}$$

The terms of the transformed compliance matrix are

$$\overline{S}_{11} = S_{11}\cos^4\theta + (2S_{12} + S_{66})\cos^2\theta\sin^2\theta + S_{22}\sin^4\theta$$

$$\overline{S}_{12} = S_{12}(\cos^4\theta + \sin^4\theta) + (S_{11} + S_{12} - S_{66})\cos^2\theta\sin^2\theta$$

$$\overline{S}_{13} = S_{13}\cos^2\theta + S_{23}\sin^2\theta$$

$$\overline{S}_{16} = (2S_{11} - 2S_{12} - S_{66})\cos^3\theta\sin\theta + (2S_{12} - 2S_{22} + S_{66})\cos\theta\sin^3\theta$$

$$S_{22} = S_{22}\cos^4\theta + (2S_{12} + S_{66})\cos^2\theta\sin^2\theta + S_{11}\sin^4\theta$$

$$\overline{S}_{23} = S_{23}\cos^2\theta + S_{13}\sin^2\theta$$

$$\overline{S}_{26} = (2S_{12} - 2S_{22} + S_{66})\cos^3\theta\sin\theta + (2S_{11} - 2S_{12} - S_{66})\cos\theta\sin^3\theta$$

$$\overline{S}_{33} = S_{33}$$

$$\overline{S}_{36} = 2(S_{13} - S_{23})\cos\theta\sin\theta$$

$$\overline{S}_{44} = S_{44}\cos^2\theta + S_{55}\sin^2\theta$$

$$\overline{S}_{45} = (S_{55} - S_{44})\cos\theta\sin\theta$$

$$\overline{S}_{55} = S_{55}\cos^2\theta + S_{44}\sin^2\theta$$

$$\overline{S}_{66} = 4(S_{11} + S_{22} - 2S_{12})\cos^2\theta\sin^2\theta + S_{66}(\cos^2\theta - \sin^2\theta)^2$$

CHAPTER FIVE

FINITE ELEMENT MODEL

5.1 Element Model Description

The finite element model used for studying the dynamic behavior of multi-layered composite plates (Figure 4.1) is an eight-noded rectangular solid thin plate element. For each node, there are three degrees of freedom, i.e., translations along the global coordinate axes of x, y, and z. The local element coordinate system (x_1, x_2, and x_3) is arranged with the first axis being coincident with the fiber direction.

5.2 Expressions for Displacement and Strain

For an eight-node finite element with three degrees of freedom per node, the displacement field over an element is given by

$$\{\delta^e\} = \sum_{i=1}^{8} [N_i]\{\delta_i\} \tag{5.1}$$

where $\{\delta_i\}$ is the displacement vector at node i and $[N_i]$ is the shape matrix.

Therefore, for an eight-node finite element with three degrees of freedom per node, the strain field over an element can be expressed as

$$\{\varepsilon^e\} = [B]\{\delta^e\} \tag{5.2}$$

where $[B]$ is the strain-displacement relation matrix. (Bathe, 1982)

5.3 Stress Strain Relationship and Equation of Motion

According to the equations (4.10) and (5.2), the stresses of an element in the global coordinate system can be expressed by the nodal displacements as

$$\{\sigma^e\} = [A][C][A]^{-1}[B]\{\delta^e\} \tag{5.3}$$

The strain energy of the k[th] element is

$$U_k^e = \frac{1}{2}\int_{Vk} \{\varepsilon^e\}^T \{\sigma^e\} dV = \frac{1}{2}\{\delta_k^e\}^T [K_k^e]\{\delta_k^e\} \tag{5.4}$$

where $\{\delta_k^e\}$ and $[K_k^e]$ represents the displacement vector and the stiffness matrix of the k[th] element, respectively. The total strain energy for a composite plate consisting of *N* elements can be expressed as

$$U = \sum_{k=1}^{N} U_k^e = \frac{1}{2}\sum_{k=1}^{N} \{\delta_k^e\}^T [K_k^e]\{\delta_k^e\} \tag{5.5}$$

Therefore, after assembly of nodal displacement of all elements, the total strain of a multi-layer composite plate can be expressed as

$$U = \frac{1}{2}\{\delta\}^T [K]\{\delta\} \tag{5.6}$$

where $\{\delta\}$ and $[K]$ are the global nodal displacement vector and stiffness matrix, respectively.

The kinetic energy of the k[th] element is

$$T_k^e = \frac{1}{2}\int_{Vk} \rho \left\{\dot{\delta}_k^e\right\}^T dV = \frac{1}{2}\left\{\dot{\delta}_k^e\right\}^T [M_k^e]\left\{\dot{\delta}_k^e\right\} \tag{5.7}$$

where $\{\dot{\delta}_k^e\}$ and $[M_k^e]$ represent the velocity vector and the mass matrix of the k[th] element, respectively. The total kinetic energy for a composite plate consisting of *N* elements can be expressed as

$$T = \sum_{k=1}^{N} T_k^e = \frac{1}{2}\sum_{k=1}^{N} \left\{\dot{\delta}_k^e\right\}^T [M_k^e]\left\{\dot{\delta}_k^e\right\} \tag{5.8}$$

Therefore, after assembly of nodal velocities of all elements, the total kinetic energy of multi-layer composite plate can be represented as

$$T = \frac{1}{2}\left\{\dot{\delta}\right\}^T [M]\left\{\dot{\delta}\right\} \tag{5.9}$$

where $\{\dot{\delta}\}$ and $[M]$ are the global nodal velocity vector and mass matrix, respectively.

If the composite plate experiences a harmonic motion with angular frequency ω, the kinetic energy of the composite plate will be

$$T = \frac{1}{2}\omega^2 \{\delta\}^T [M] \{\delta\} \tag{5.10}$$

Then, using the Lagrange's principle the equation of motion free vibration of the composite plate is reduced to the eigenvalue problem of

$$\left([K] - \omega^2 [M]\right)\{\delta\} = 0 \tag{5.11}$$

CHAPTER SIX

PROBLEM DEFINITION

6.1 Finite Element Models of Laminated Composite Plates

This section describes the three-dimensional finite element models of laminated composite plates are used in this study. These are intact model (Plate 0) and delaminated models having different delamination types such as circular strip delamination (Plate A), circular hole delamination (Plate B) and the circular strip delamination around a circular hole delamination (Plate C).

Three-dimensional finite element Plate 0 and Plate B are designed as sixteen volumes. Eight volumes of them are at the top region and other eight volumes are at the bottom region. The areas of A1, A2, A3, A4, A5, A6, A7, A8 were the common areas of the top and bottom volumes.

Figure 6.1 shows the common areas of intact model, Plate 0, and Figure 6.2 shows the common areas of the circular hole delaminated model, Plate B.

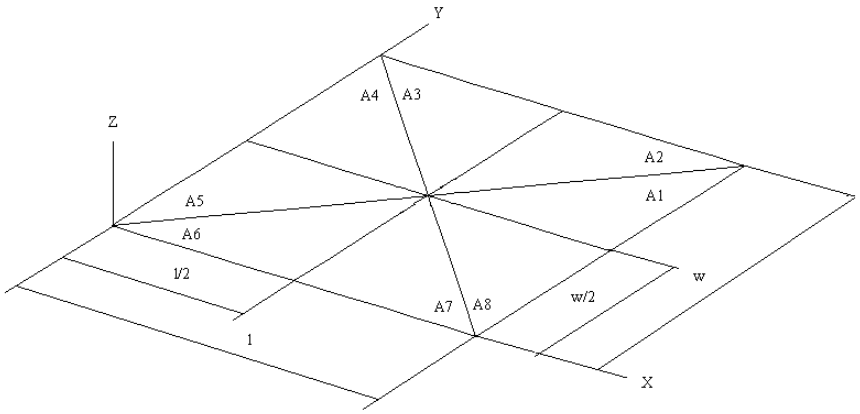

Figure 6.1 The common areas of Plate 0

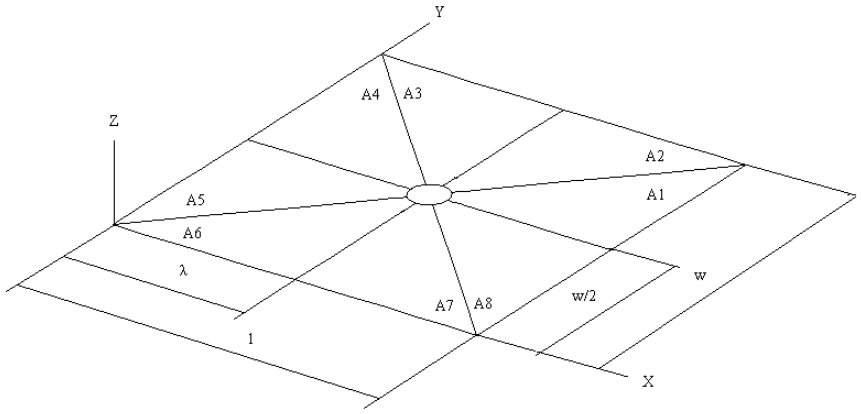

Figure 6.2 The common areas of Plate B

Three-dimensional finite element model of Plate A and Plate C are designed as thirty-two volumes. Sixteen volumes of them are at the top region and other sixteen volumes are at the bottom region. In this design, some areas in the interfaces of this top and bottom volumes are not same although these areas has the same dimensions and coordinates. In such a manner that, while the areas of A9, A10, A11, A12, A13, A14, A15, A16 belong to the bottom volumes , the areas of A17, A18, A19, A20, A21, A22, A23, A24 which have the same dimensions and coordinates with above areas belong to the upper volumes.

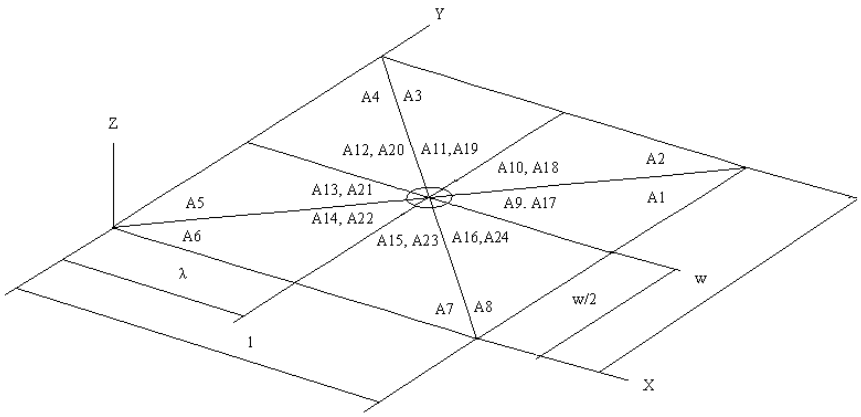

Figure 6.3 The interfacial areas of Plate A

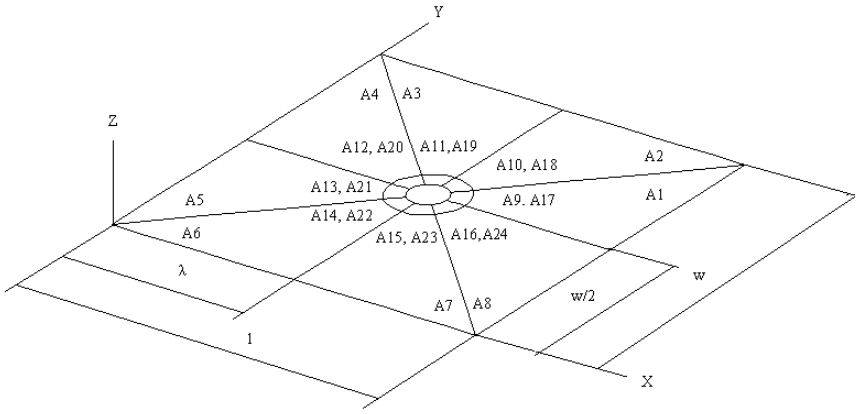

Figure 6.4 The interfacial areas of Plate C

Nevertheless, the areas of A1, A2, A3, A4, A5, A6, A7, A8 were the common areas of the top and bottom volumes of the Plate A and Plate C. Due to the top and bottom volumes do not glue in the interfacial areas, when the volumes mesh, double nodes occur at the same coordinates of the interfacial areas.

Figure 6.3 shows the interfacial and common areas of circular strip delaminated model, Plate A, and Figure 6.4 shows the interfacial and common areas of the circular strip delaminated around a circular delamination model, Plate C.

6.2 Statement of the Problem

In this thesis, it is purposed to investigate the dynamic responses of laminated composite plates, which are subjected to delamination. Especially, effects of delamination width and location on the natural frequency of both clamped-free and clamped-pinned laminated composite plates and in addition to these, harmonic response of a clamped-free laminated composite plate, which have a circular strip delamination around a circular hole delamination, are investigated. For this purpose, parametric input files are developed by using ANSYS software in order to determine the natural frequencies and associated mode shapes with the harmonic responses of the laminated composite plates.

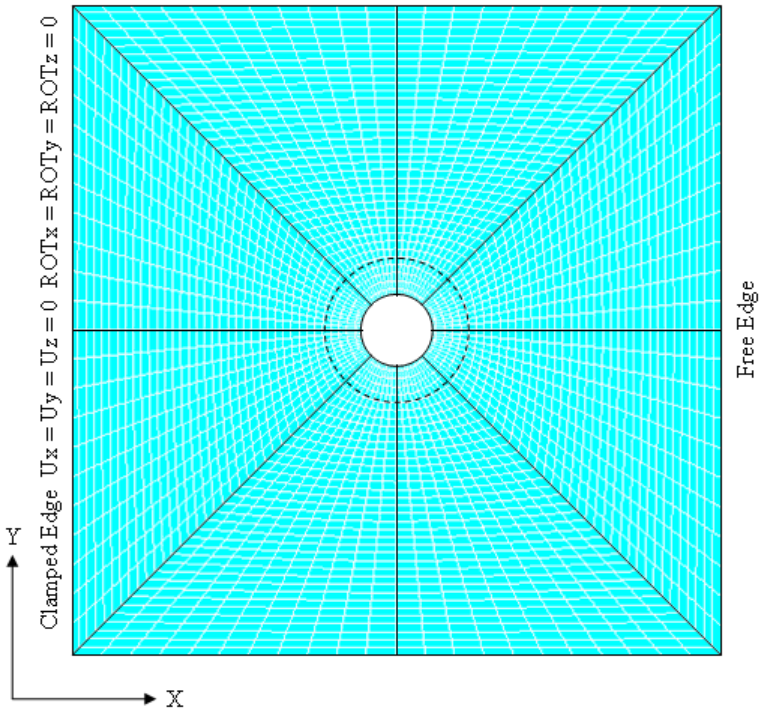

Figure 6.5 Boundary conditions of the clamped-free plates

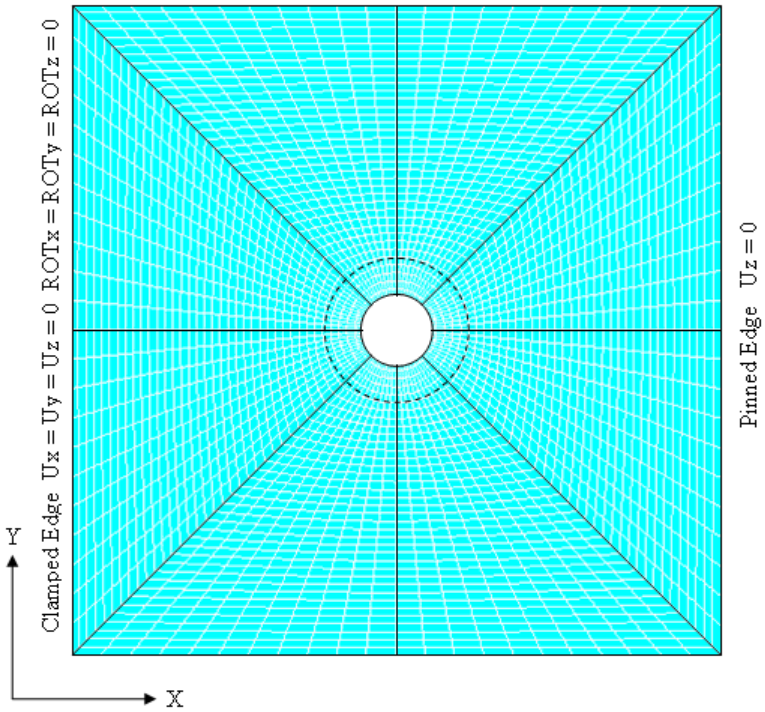

Figure 6.6 Boundary conditions of the clamped-pinned plates

CHAPTER SEVEN

MODEL REFINEMENT AND VERIFICATION

7.1 Model Refinement

The element size has a major significance on the accuracy of the finite element results. In case of the element size decreases, accuracy of the finite element analysis results increases, but at the same time, the solution time increases with that. Herein, selecting of the element size, which gives high accuracy with the minimum solution time is important.

A six layer laminated square composite plate with a side length of 178mm and a total thickness of 1.58mm is considered. All the ply orientations are equal to 0^0 and the elasticity modules are E_1=72.7GPa, $E_2=E_3$=7.2GPa, shear modules are $G_{12}=G_{13}$=3.76GPa, G_{23}=2.71GPa, poisson's ratios are $\upsilon_{12}=\upsilon_{13}$=0.3, υ_{23}=0.33 and density is ρ=1566kgm^{-3}, Lin et al. (1984), Yam et al. (2004), and Alnefaie (2009).

Table 7.1 Natural frequencies (Hz) of the intact $[0^0/0^0/0^0/0^0]_s$ free plate with a side length of 178mm and a total thickness of 1.58mm using different meshes.

Mode	Number of elements for each lamina				
	25	100	200	2000	8000
1	82.75	81.88	81.65	81.52	81.46
2	111.62	110.43	110.03	109.92	109.90
3	217.79	202.42	200.12	199.57	199.38
4	320.93	308.34	304.18	303.01	302.85
5	465.17	403.69	394.00	392.06	391.65

Table 7.1 shows the natural frequencies of the first five modes for different generated mesh sizes. A remarkable change in results is obtained when increasing the total number of elements from 25 to 200 elements per layer. Meanwhile, the change in natural frequency obtained with 8000 elements in comparison with 2000 is negligible. This leads to applying the 2000 elements per layer for each lamina model in the subsequent computations to achieve high accuracy and minimum computations time.

7.2 Model Verification with Results in Literature

To verify the results of the developed model in Section 7.1, the results obtained here are compared with experimental work of Lin et al. (1984) and the numerical results of Yam et al. (2004), and Alnefaie (2009). Table 7.2 shows the natural frequencies for the first five modes of the present analysis and the reported results. The present analysis shows close results to the reported results.

Table 7.2 Natural frequencies (Hz) of the intact $[0^0/0^0/0^0/0^0]_s$ free plate

Mode	Present	Alnefaie (2009)	Yam et al. (2004)	Lin et al. (1984)
		Numerical	Numerical	Experimental
1	81.52	81.48	82.26	81.50
2	109.92	109.20	113.10	107.40
3	199.57	199.50	207.29	196.60
4	303.01	300.46	325.28	285.50
5	392.06	391.40	408.51	382.50

In addition to this verification, another laminated composite plate, which has a sixteen-layer with an area of 240x180mm^2 and a thickness of 2.08mm, is considered. The ply orientations are $[0^0/0^0/90^0/90^0/0^0/0^0/90^0/90^0]_s$, elasticity modules are E_1=125GPa, E_2=E_3=8.5GPa, shear modules are G_{12}=G_{13}=4.5GPa, G_{23}=3.27GPa, poisson's ratios are υ_{12}=υ_{13}= υ_{23}=0.3 and density is ρ=1550kgm^{-3}, Wei et al. (2004) and Alnefaie (2009). The first five natural frequencies of this plate are compared with the numerical results and the reported results. Table 7.3 shows the natural frequencies for the first five modes of the present analysis and the reported results. Again, the present model demonstrates better agreement with the reported results.

Table 7.3 Natural frequencies (Hz) of the intact $[0^0/0^0/90^0/90^0/0^0/0^0/90^0/90^0]_s$ free plate

Mode	Present	Alnefaie (2009)	Wei et al. (2004)	
		Numerical	Numerical	Experimental
1	88.43	89.16	90.53	90
2	280.89	278.97	279.18	289
3	332.87	330.35	333.60	318
4	356.16	354.92	354.23	354
5	397.61	393.26	397.63	386

7.3 Model Verification with Results of Experimental Study

In this section, free vibration response of the clamped-free laminated woven composite beams, which have an area of 270x22mm^2 and a thickness of 2.5mm, are measured by a laser displacement meter and these results are compared with the numerical results, which are obtained with the finite element analysis. Four laminated composite beams are considered. One of that is intact, and the other beams have a circular delamination around a circular hole delamination located at different positions. Delamination center locations from the clamped edge are 20mm, 40mm and 80mm in the delaminated composite beams. In finite element analysis, diameters of the circular hole delamination and the circular strip delamination of these delaminated beams are assumed equal and 5mm and 10mm, respectively.

All the ply orientations are equal to 0^0 and elasticity modules are $E_1=E_2=22.32$GPa, $E_3=13.392$GPa, shear modules are $G_{12}=3.08$GPa, $G_{13}=G_{23}=1$GPa, poisson's ratios are $\upsilon_{12}=0.16$, $\upsilon_{13}=\upsilon_{23}= 0.15$ and density is $\rho=1830$kgm^{-3}.

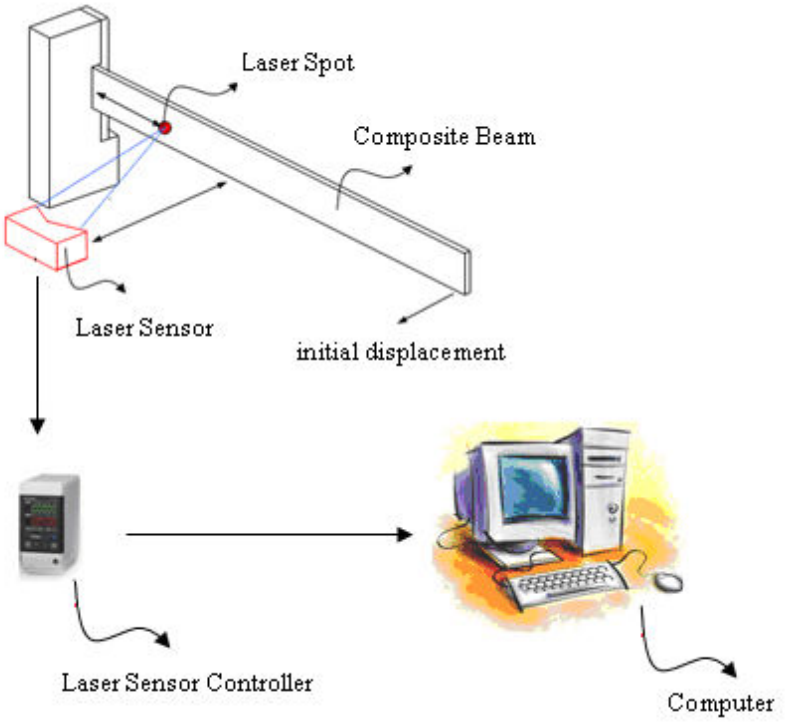

Figure 7.1 Schematic view of experimental setup

Schematic view of the experimental setup is shown in Figure 7.1. The Keyence LKG150 laser displacement sensor and its controller are used to measure the free vibration response of the beam. Free vibration response of the beam is initiated by giving 20mm initial displacement at the tip. The free displacement response of the beam is measured by the laser sensor for the point 50mm away from the root clamped end.

The free vibration responses of intact and delaminated beams are given in figures, which are from Figure 7.2 to Figure 7.5. The fast Fourier transform of the free displacement response gives the natural frequency of the beam. Figure 7.2 shows the free displacement response and its frequency content of the intact beam. The first natural frequency of the intact composite beam is obtained as 16.24Hz. Figure 7.3 shows the free displacement response of the beam with a delamination located 20mm from the root. The natural frequency for this case is obtained as 15.99Hz. A small decrease is observed in the first natural frequency due to the delamination. The free displacement responses for the beams having delaminations located at 40mm and 80mm are given in Figure 7.4 and Figure 7.5. As seen from these figures that the first natural frequencies are the same with the intact composite beam. The experimental results show that the delamination has an influence on the natural frequency of the beam when the delamination closes to the clamped end of the beam.

Table 7.4 Comparisons of the numerical and experimental results for the first natural frequencies (Hz) of clamped-free beams

	Numerical	Experimental
Intact Model	19.359	16.24
λ	10mm Circular Strip Delamination around 5mm Circular Hole Delamination	
20mm	18.735	15.99
40mm	18.859	16.24
80mm	19.075	16.24

Table 7.4 lists the first natural frequencies of the clamped-free laminated composite beams for the different location of delamination. Again, the present model demonstrates better agreement with the experimental results.

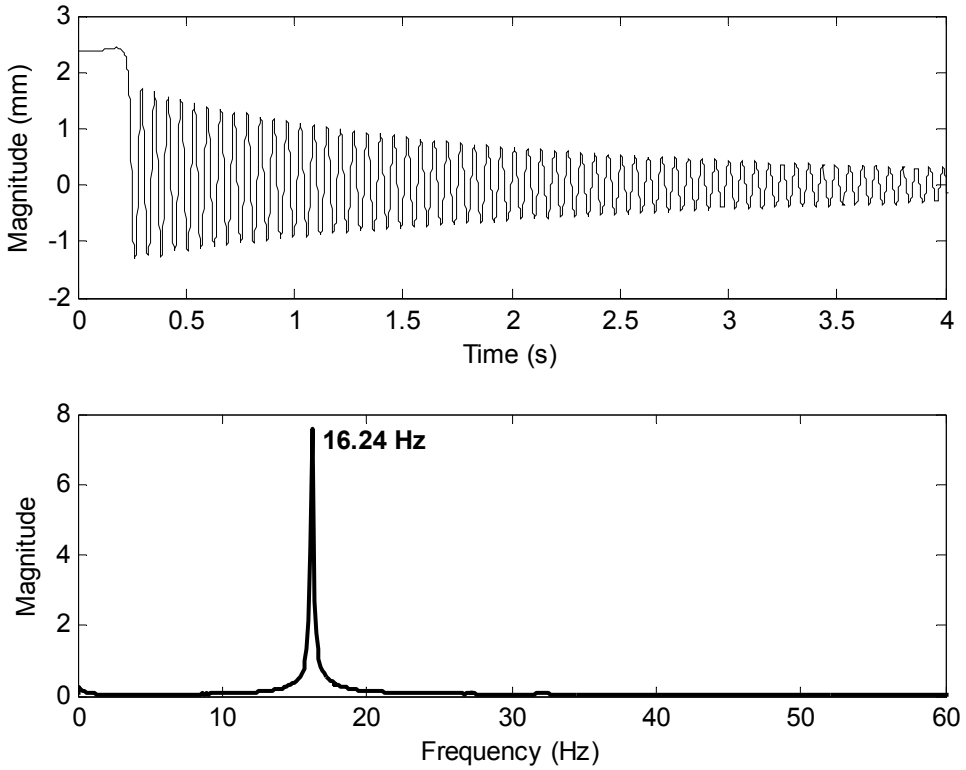

Figure 7.2 Free vibration response of the intact composite beam.

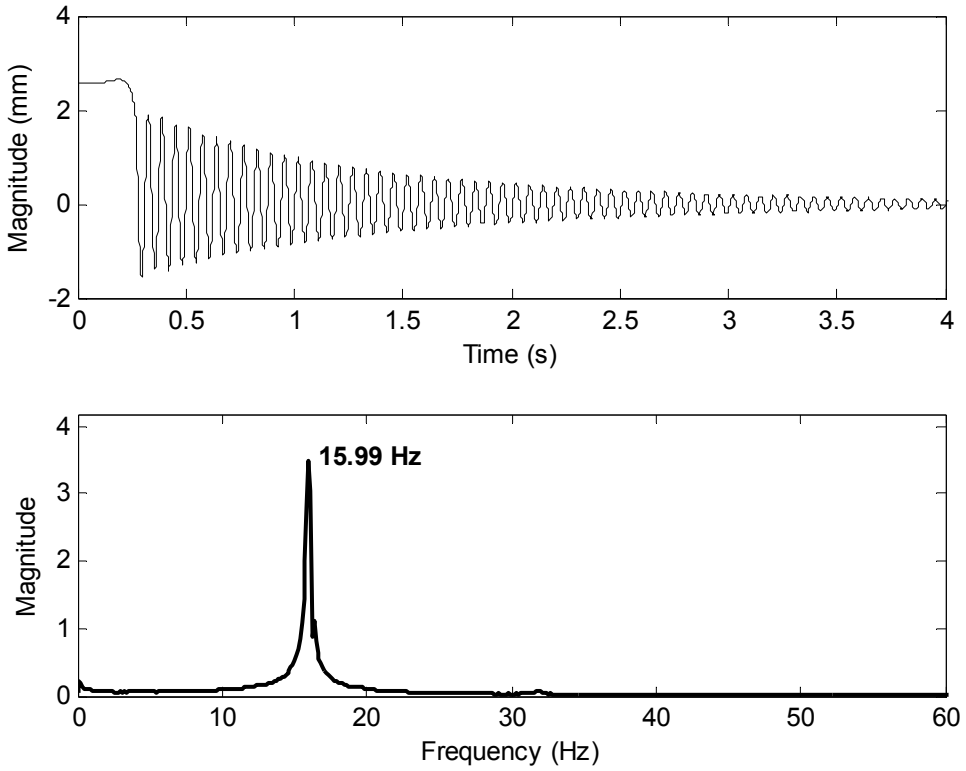

Figure 7.3 Free vibration response of the composite beam, delamination at 20mm.

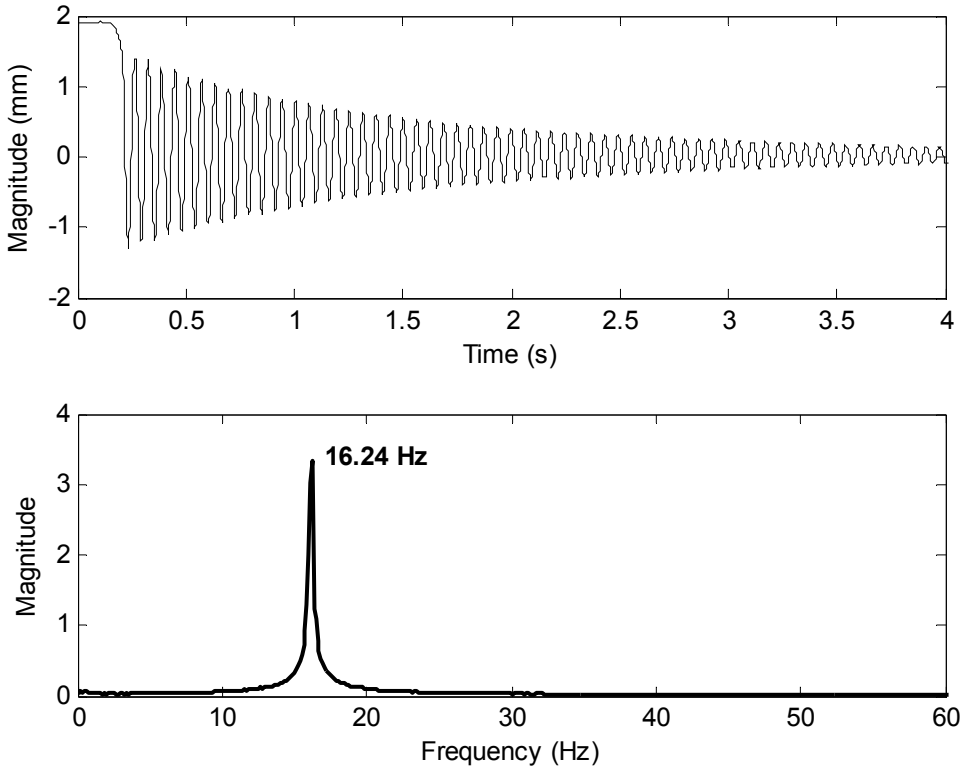

Figure 7.4 Free vibration response of the composite beam, delamination at 40mm.

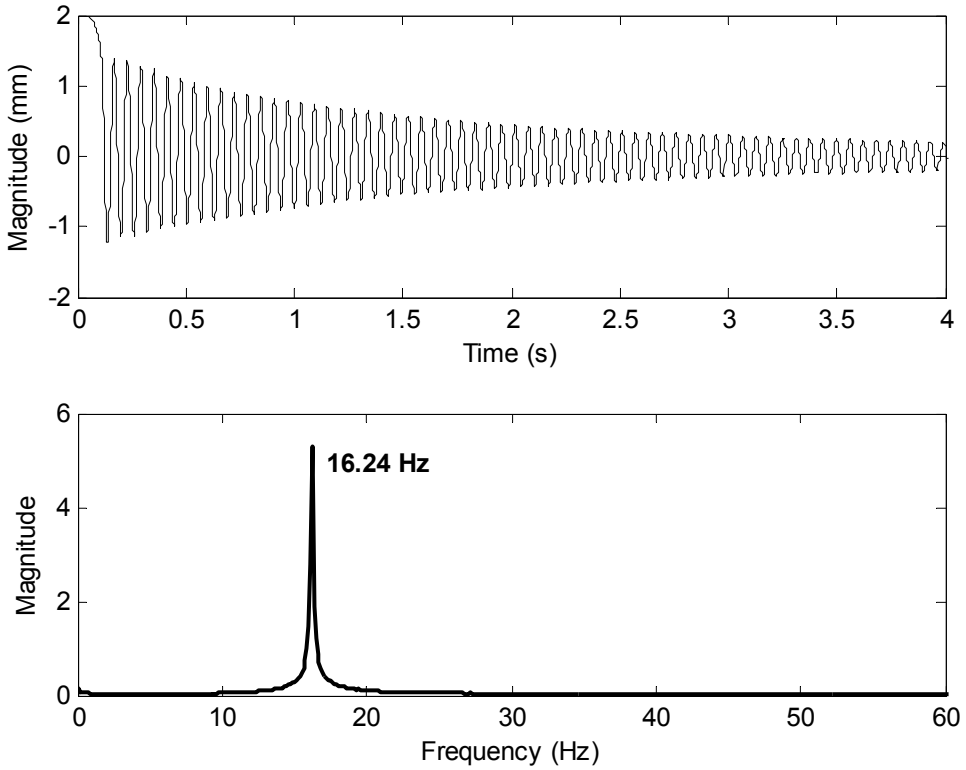

Figure 7.5 Free vibration response of the composite beam, delamination at 80mm.

CHAPTER EIGHT

RESULTS AND DISCUSSIONS

8.1 Samples

In this thesis, parametric input files are developed by using ANSYS software in order to determine the natural frequencies and associated mode shapes with the harmonic responses of the laminated composite plates. There-dimensional finite element models of laminated composite plates are formed and effects of delamination width and location on the natural frequency of both clamped-free and clamped-pinned laminated composite plates are determined. In addition to these, harmonic response of a clamped-free laminated composite plate, which have a circular strip delamination around a circular hole delamination, is investigated.

An eight-laminated composite plate with an area of 200x200mm^2 and the total thickness of 2.4mm is considered. All the ply orientations are equal to 0^0 and elasticity modules are $E_1=E_2=22.32$GPa, $E_3=13.392$GPa, shear modules are $G_{12}=3.08$GPa, $G_{13}=G_{23}=1$GPa, poisson's ratios are $\upsilon_{12}=0.16$, $\upsilon_{13}=\upsilon_{23}= 0.15$ and density is $\rho=1830$kgm^{-3}

Three-dimensional finite element models of various laminated composite plates are used in this study. These are intact model (Plate 0) and delaminated models having different delamination types such as circular strip delamination (Plate A), circular hole delamination (Plate B) and the circular strip delamination around a circular hole delamination (Plate C).

8.2 Bending Mode Shapes of the Intact Model

In this section, the first eight mode shapes of both clamped-free and clamped-pinned of the intact composite plate model are investigated, but only the first three bending mode shapes are presented. Figure 8.1, Figure 8.2, and Figure 8.3 show the

first three bending mode shapes of the clamped-free intact composite plate model, respectively, and Figure 8.4, Figure 8.5, and Figure 8.6 show the first three bending mode shapes of the clamped-pinned intact composite plate model, respectively.

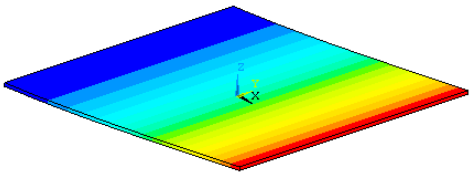

Figure 8.1 The 1st bending mode shape of CF

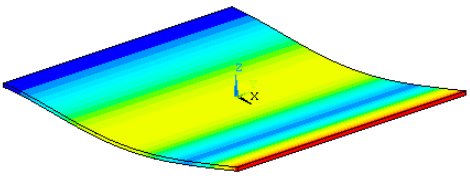

Figure 8.2 The 2nd bending mode shape of CF

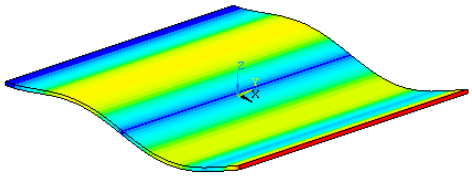

Figure 8.3 The 3rd bending mode shape of CF

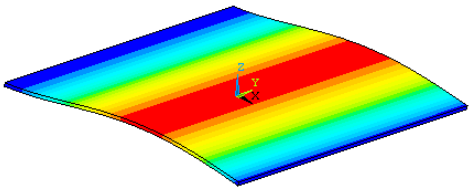

Figure 8.4 The 1st bending mode shape of CP

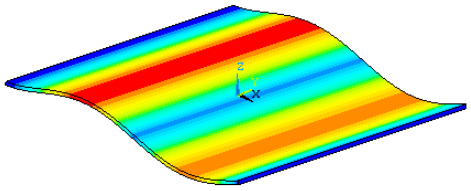

Figure 8.5 The 2nd bending mode shape of CP

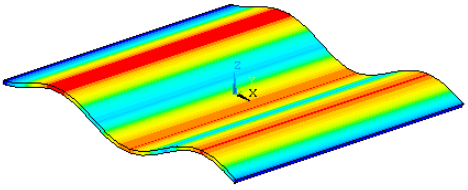

Figure 8.6 The 3rd bending mode shape of CP

8.3 Effect of Delamination on Natural Frequency

In this section, the effect of the delamination on the natural frequency of the laminated composite plate is examined. Three laminated composite plates are considered. One of the plates is intact and named 0, the other plates are named A, B, respectively, are damaged with delamination of different types. Plate A has a circular strip delamination located at the center of the plate between the fourth and fifth layers counting from the bottom of the plate. Plate B has a circular hole delamination located at the center of the plate. Plate A has a 20mm circular strip delamination, Plate B has a 20mm circular hole delamination. The first eight natural frequencies of both clamped-free and clamped-pinned laminated composite plates are determined.

Table 8.1 Numerical results of the natural frequencies (Hz) for the clamped-free plate

	Intact Model	Circular Strip Delamination	Circular Hole Delamination
		Diameter 20 mm	Diameter 20 mm
Mode	Plate 0	Plate A	Plate B
1	34.293	34.277	34.162
2	111.33	111.13	110.68
3	215.30	214.51	211.53
4	274.98	274.05	272.64
5	397.43	395.10	389.96
6	523.62	519.40	508.73
7	605.86	599.37	592.68
8	654.76	651.04	641.39

Table 8.2 Numerical results of the natural frequencies (Hz) for the clamped-pinned plate

	Intact Model	Circular Strip Delamination	Circular Hole Delamination
		Diameter 20 mm	Diameter 20 mm
Mode	Plate 0	Plate A	Plate B
1	150.65	150.15	149.05
2	202.82	202.15	201.38
3	457.16	452.45	443.49
4	490.57	485.54	480.55
5	533.12	530.03	523.01
6	726.46	718.58	710.39
7	935.96	912.72	903.02
8	1031.9	1010.4	988.61

Table 8.1 lists the natural frequencies for the clamped-free plates with different types of delamination and Table 8.2 lists the natural frequencies for the clamped-pinned plates with different types of delamination.

It can be seen that in the existence of delamination, the natural frequency decreases. It is also seen that decrease of the natural frequencies is not the same for different modes.

8.4 Effect of Delamination Width on Natural Frequency

In this section, the effect of the delamination width on the natural frequency of the laminated composite plate is examined. Ten laminated composite plates are considered. One of the plates is intact and named 0. The other plates have a circular strip delamination located at the center of the plate between the fourth and fifth layers counting from the bottom of the plate. In this study, dw indicates ratio of the delamination diameter to the plate length. The diameter of the circular strip delamination is changed to 20mm, 30mm, 40mm, 50mm, 60mm, 70mm, 80mm, 90mm, and 100mm, respectively.

Table 8.3 Numerical results of the first eight natural frequencies (Hz) for different delamination width for the clamped-free plate

	Intact Model	Circular Strip Delamination								
		dw								
Mode	Plate 0	0,1	0,15	0,2	0,25	0,3	0,35	0,4	0,45	0,5
1	34.293	34.277	34.270	34.261	34.243	34.214	34.163	34.089	33.982	33.836
2	111.33	111.13	111.02	110.96	110.88	110.74	110.52	110.21	109.74	109.11
3	215.30	214.51	214.19	214.28	213.98	213.86	213.61	213.19	212.46	211.28
4	274.98	274.05	273.47	273.11	272.59	271.81	270.64	269.04	266.96	264.43
5	397.43	395.10	393.68	393.21	392.82	392.32	391.49	390.02	387.50	383.40
6	523.62	519.40	518.29	517.79	517.06	515.70	512.81	507.54	498.53	484.97
7	605.86	599.37	595.79	592.11	585.85	575.94	561.92	544.92	527.09	510.88
8	654.76	651.04	646.91	645.62	644.61	643.38	641.28	637.61	631.55	622.29

Table 8.4 Numerical results of the first eight natural frequencies (Hz) for different delamination width for the clamped-pinned plate

	Intact Model	Circular Strip Delamination								
		dw								
Mode	Plate 0	0,1	0,15	0,2	0,25	0,3	0,35	0,4	0,45	0,5
1	150.65	150.15	149.95	149.84	149.71	149.50	149.14	148.60	147.81	146.68
2	202.82	202.15	201.85	201.58	201.15	200.46	199.39	197.88	195.86	193.34
3	457.16	452.45	452.18	451.95	451.42	450.26	447.70	442.90	434.46	422.47
4	490.57	485.54	483.20	481.08	477.58	472.03	463.95	453.64	441.94	429.03
5	533.12	530.03	527.15	526.23	525.50	524.62	523.17	520.73	516.79	510.86
6	726.46	718.58	715.07	710.91	704.06	694.43	682.74	670.90	660.05	650.43
7	935.96	912.72	906.52	893.87	871.65	840.60	804.39	768.98	737.64	692.58
8	1031.9	1010.4	1003.3	999.51	994.12	984.72	966.91	936.79	849.47	711.94

The natural frequencies are computed for the first eight modes of both clamped-free and clamped-pinned laminated composite plates. Table 8.3 and Table 8.4 list the natural frequencies for the clamped-free and clamped-pinned laminated composite plates with different width of central strip delamination, respectively. It can be seen that the natural frequencies decrease with the increase of delamination width.

The relationship between the frequency and delamination width is investigated. Figures, which are from Figure 8.7 to Figure 8.12, show the percentage changes in the first eight natural frequencies as a function of the delamination width, where the height of the column represents the absolute value of the percentage change of natural frequency, i.e.

$$\kappa = \frac{\left|\omega_{\text{delaminated}} - \omega_{\text{intact}}\right|}{\omega_{\text{intact}}} \times 100$$

Figure 8.7 and Figure 8.9 show the percentage changes in natural frequencies for the first five modes as a function of delamination width for the clamped-free and clamped-pinned plate, respectively, and Figure 8.8 and Figure 8.10 show the percentage changes in natural frequencies for the higher other modes as a function of delamination width for the clamped-free and clamped-pinned plate, respectively.

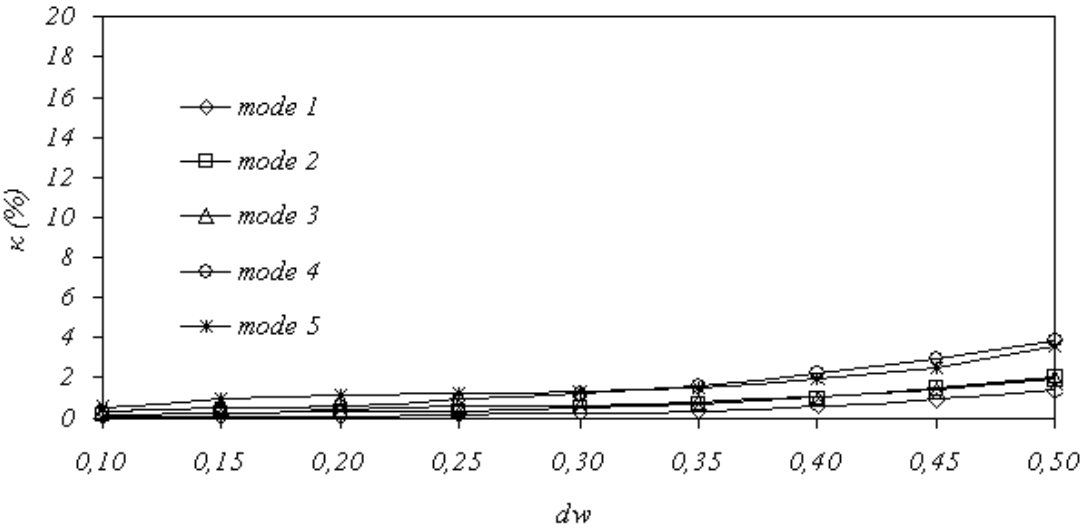

Figure 8.7 Percentage changes of the natural frequencies for clamped-free plates with delamination of different widths for modes 1–5.

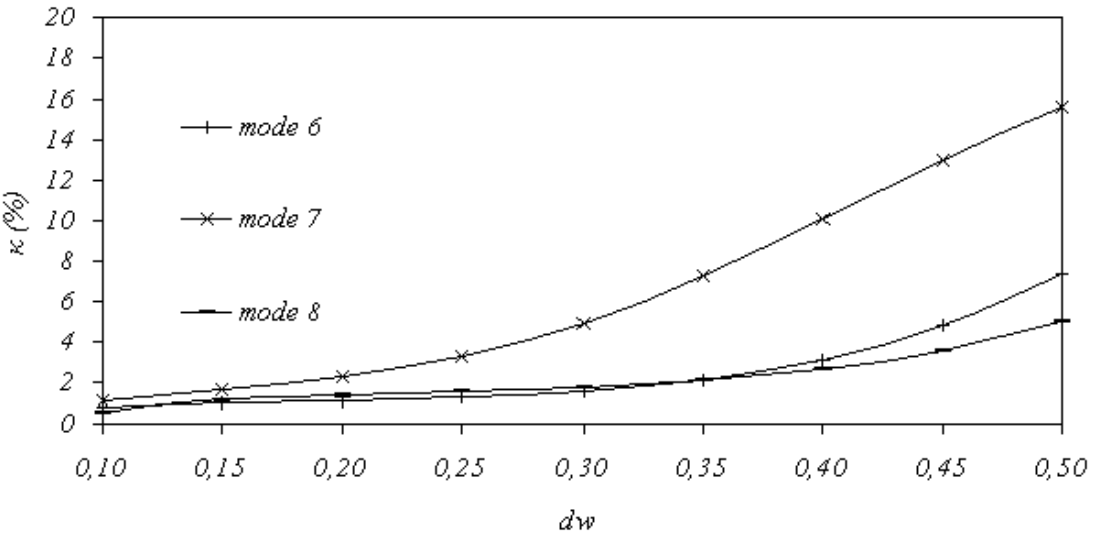

Figure 8.8 Percentage changes of the natural frequencies for clamped-free plates with delamination of different widths for modes 6–8

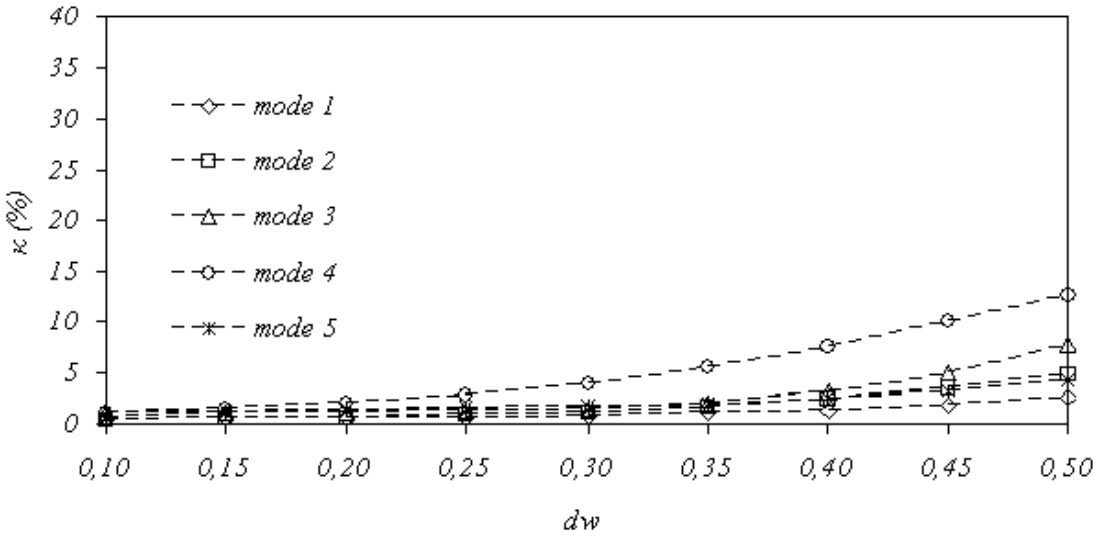

Figure 8.9 Percentage changes of the natural frequencies for clamped-pinned plates with delamination of different widths for modes 1–5.

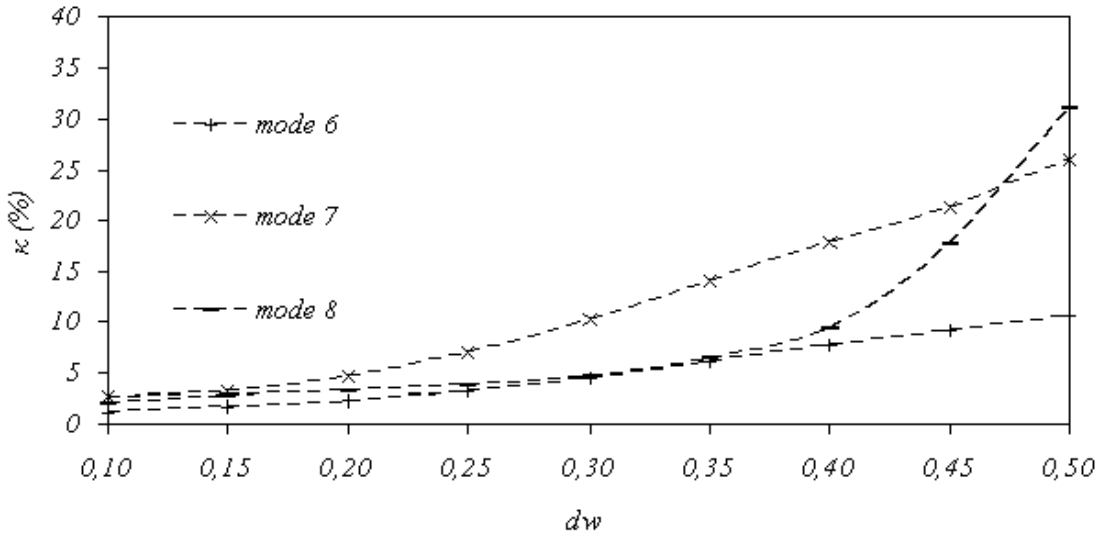

Figure 8.10 Percentage changes of the natural frequencies for clamped-pinned plates with delamination of different widths for modes 6–8

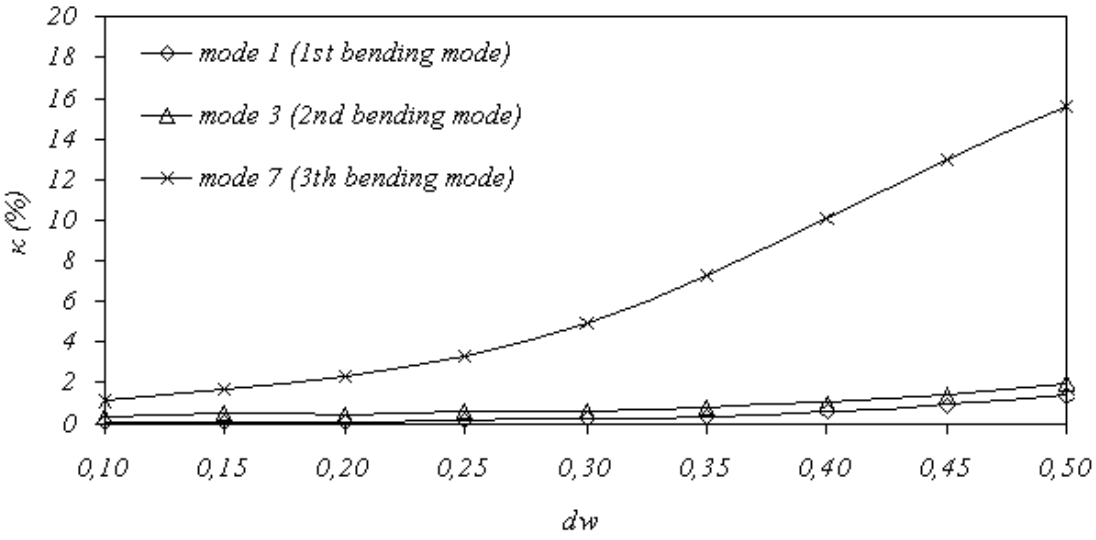

Figure 8.11 Percentage changes of the first three bending natural frequencies for clamped-free plates with delamination of different widths

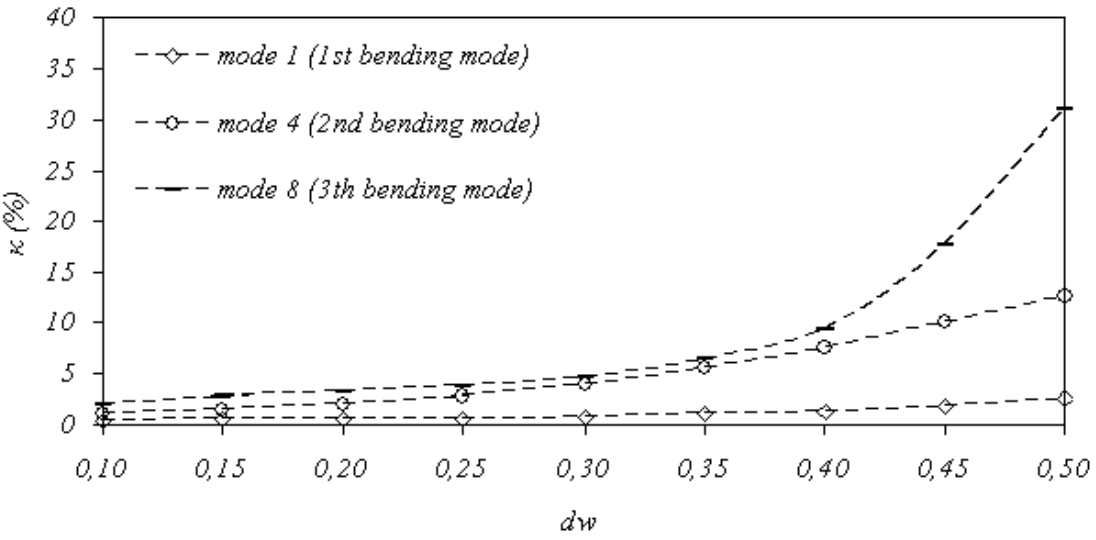

Figure 8.12 Percentage changes of the first three bending natural frequencies for clamped-pinned plates with delamination of different widths

It is noticed that the percentage changes in the natural frequencies increase with the increase of delamination width. It is seen that the decrease of the natural frequencies is not the same for different modes. From Figure 8.7, Figure 8.8 and Figure 8.9, Figure 8.10 for the clamped-free and clamped-pinned plates, respectively, it is also seen that effect of delamination width on the natural frequencies is very small for the five fist modes and high for the other modes.

Figure 8.11 and Figure 8.12 show the percentage changes in the first three bending natural frequencies as a function of the delamination width. From Figure 8.11, it is seen that decrease of the natural frequencies is relatively large for mode 7, which is the third bending mode of the clamped-free plate, and the change of the natural frequencies is almost negligible in mode 1 and mode 3, which are the first and second bending modes of the clamped-free plate, respectively. From Figure 8.12, it seen that decrease of the natural frequencies is relatively large for mode 4 and mode 8, which are the second and third bending modes of the clamped-pinned plate, respectively, and the change of the natural frequencies is almost negligible in mode 1, which is the first bending mode of the clamped-pinned plate.

The variation manner of the values is not the same for each plate. The changes of the natural frequencies are nearly zero for all the considered cases while the delamination width ratio dw is smaller than a certain value. However, the changes of the natural frequencies are high for all the considered cases while the delamination width ratio dw is higher than a certain value. These indicate that the frequency change is insignificant for small delamination while significant for large delamination.

Therefore, it is indispensable to analyze the changes of other parameters such mode shapes, modal strains, etc., for effective detection of frequency changes in delaminated composite plates.

8.5 Effect of Delamination Location on Natural Frequency

In this section, the effect of the delamination location on the first and second bending natural frequency of the laminated composite palate is examined. Eighteen laminated composite plates are considered. One of that is intact, and the other plates have a circular hole delamination located at different positions. In this study, λ/l indicates ratio of the delamination center location to the plate length. The diameter of hole delamination are selected 20mm (dw 0.10) and 30mm (dw 0.15).

The natural frequencies are computed for the first two bending modes of both clamped-free and clamped-pinned laminated composite plates. Table 8.5 and Table 8.6 list the natural frequencies for the clamped-free and clamped-pinned laminated composite plates with different location of delamination, respectively.

Table 8.5 Numerical results of the first two bending natural frequencies (Hz) for clamped-free plate

	Bending Mode			
	1	2	1	2
Plate 0	34.293	215.30	34.293	215.30
λ/l	dw 0.10		dw 0.15	
0.10	33.398	211.58	32.547	209.65
0.15	33.459	212.83	32.650	211.36
0.20	33.567	213.67	32.807	212.95
0.25	33.682	213.94	33.019	213.69
0.30	33.794	213.74	33.242	213.57
0.35	33.899	213.23	33.459	212.82
0.40	33.995	212.60	33.662	211.76
0.45	34.082	212.00	33.852	210.66
0.50	34.162	211.53	34.026	209.74
0.55	34.235	211.27	34.189	209.13
0.60	34.303	211.24	34.340	208.90
0.65	34.366	211.43	34.485	209.06
0.70	34.428	211.79	34.626	209.60
0.75	34.486	212.27	34.762	210.46
0.80	34.547	212.89	34.903	211.70
0.85	34.609	213.63	35.049	213.36
0.90	34.674	214.55	35.203	215.49

Table 8.6 Numerical results of the first two bending natural frequencies (Hz) for clamped-pinned plate

	Bending Mode			
	1	2	1	2
Plate 0	150.65	490.57	150.65	490.57
λ/l	dw 0.10		dw 0.15	
0.10	147.78	479.14	146.18	475.85
0.15	148.64	481.28	147.34	478.74
0.20	149.35	481.75	148.65	480.82
0.25	149.78	480.97	149.57	481.06
0.30	149.94	479.87	149.99	480.19
0.35	149.87	479.22	149.98	479.14
0.40	149.65	479.30	149.66	478.49
0.45	149.35	479.90	149.17	478.32
0.50	149.05	480.55	148.63	478.34
0.55	148.80	480.80	148.16	478.20
0.60	148.64	480.40	147.84	477.69
0.65	148.59	479.47	147.70	476.85
0.70	148.64	478.40	147.74	475.96
0.75	148.78	477.63	147.93	475.23
0.80	148.99	477.54	148.23	475.05
0.85	149.21	478.15	148.59	475.42
0.90	149.41	479.18	148.95	476.32

Figures, which are from Figure 8.13 to Figure 8.16, show the normalized natural frequencies as a function of the delamination location, where the height of the column represents the normalized natural frequency, i.e.

$$\xi = \frac{\omega_{\text{delaminated}}}{\omega_{\text{intact}}}$$

It is seen that the decrease of the natural frequencies is not the same for different location of delamination. Comparison of the natural frequencies of the different delamination location with its width can be seen in figures, which are from Figure 8.13 to Figure 8.16. Continuous and dotted lines indicate the boundary condition of clamped-free and clamped-pinned, respectively. From the results presented in these figures, it can be seen delamination location has significant effect with its width on the free vibration. Changing level of the natural frequencies with the delamination location increases with the increase of the delamination width.

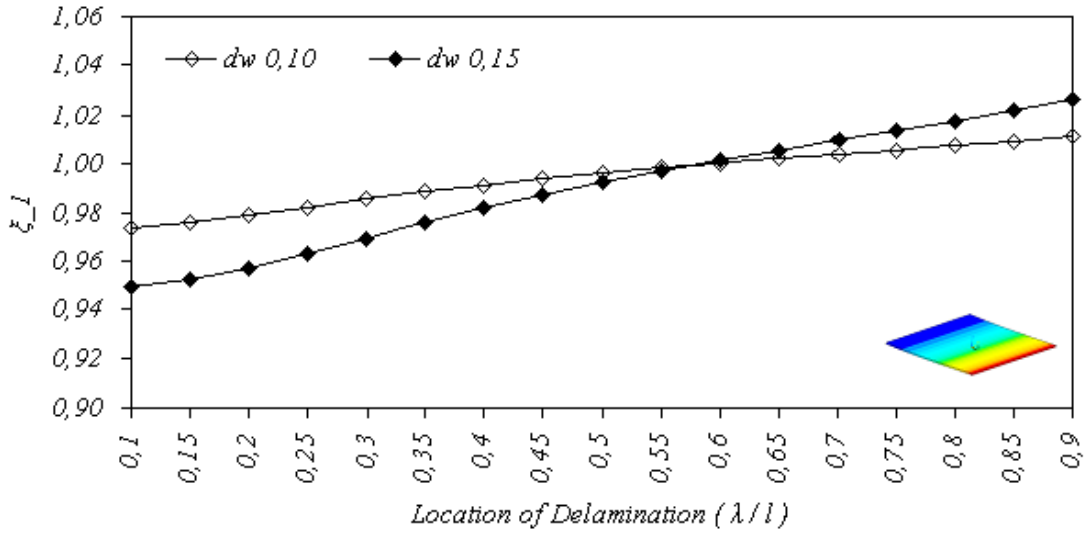

Figure 8.13 Effect of the delamination location on the normalized first natural bending frequency of clamped-free plate

The first bending natural frequency of the clamped-free plate is close to that of intact plate when the delamination is in the close vicinity of the free end of the plate. The second bending natural frequency of the clamped-free plate is minimum where the delamination is at λ/l=0.60, which is the most elastic location of the second bending mode shape.

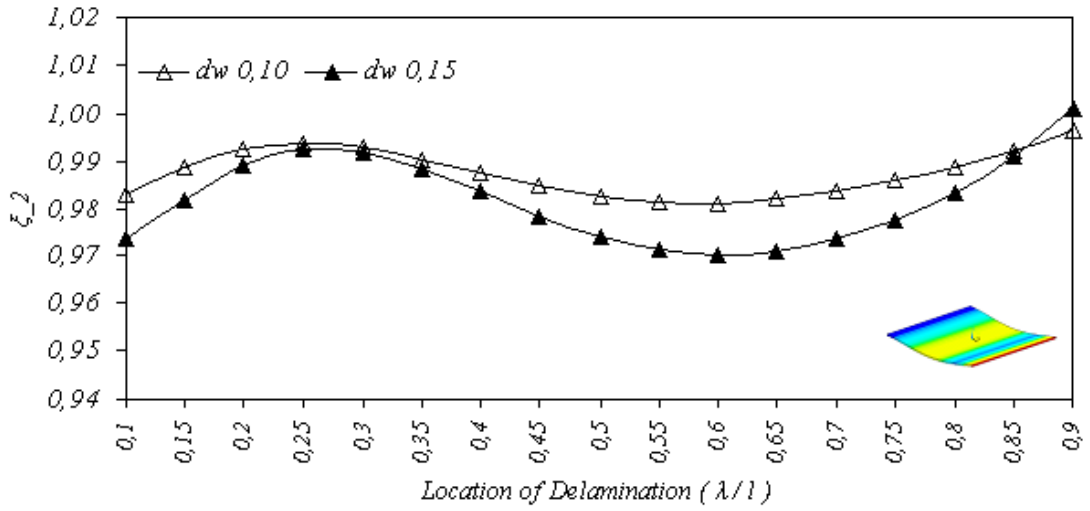

Figure 8.14 Effect of the delamination location on the normalized second natural bending frequency of clamped-free plate

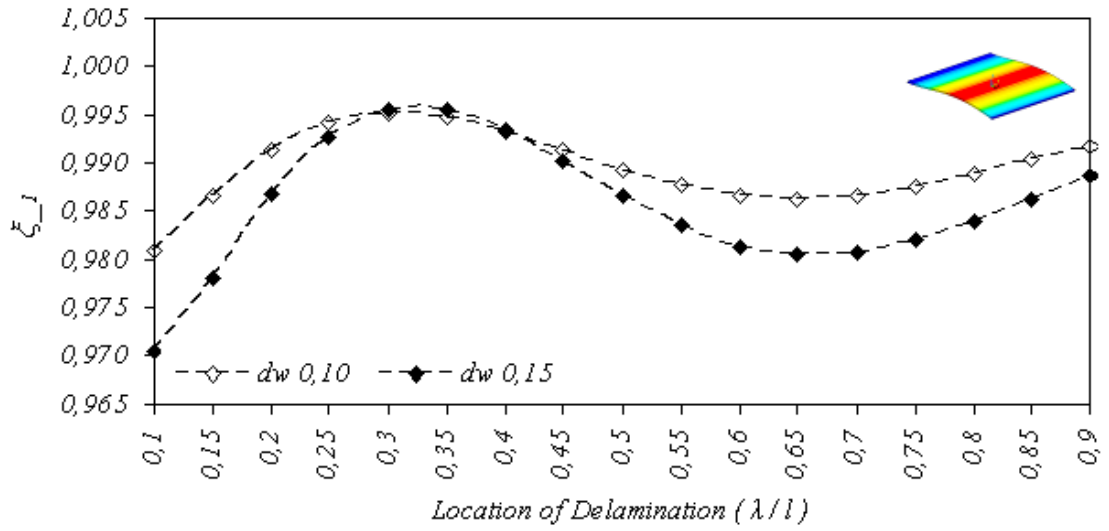

Figure 8.15 Effect of the delamination location on the normalized first natural bending frequency for clamped-pinned plate

The first bending natural frequency of the clamped-pinned plate is minimum where the delamination is at λ/l=0.65 and the second bending natural frequency of the clamped-pinned plate is minimum where the delamination is at λ/l=0.80.

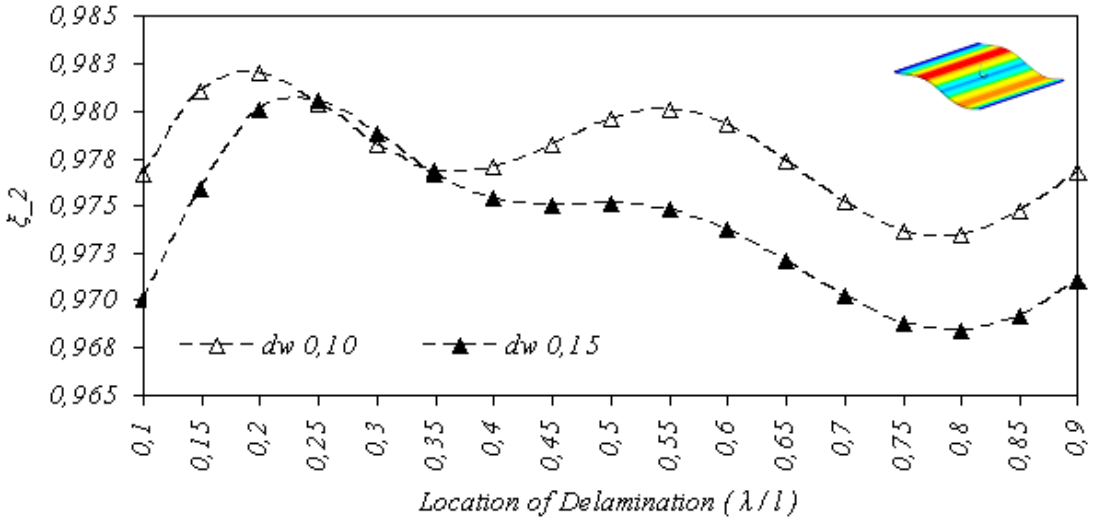

Figure 8.16 Effect of the delamination location on the normalized second natural bending frequency for clamped-pinned plate

From the results presented in these figures, it can be seen that natural frequency is significantly influenced by the location and width of delamination. Also seen from the figures is that natural frequency increases as the delamination moves away along the axial direction from the clamped edge, and decreases as the delamination closes to twist point, and then increases again as the delamination moves away along the axial direction from the twist point of the plate. Also seen that the natural frequencies are minimum at different certain points for each bending mode and boundary conditions. This condition occurs due to the shape of the bending mode.

8.6 Harmonic Analysis

Harmonic analysis is still used widely in vibration simulation and testing. Harmonic response reveals dynamic parameters of the structures such as natural frequency, damping, etc. Harmonic analysis is used to calculate the peak steady state response due to harmonic loads. Peak harmonic response occurs at forcing frequencies that match the natural frequencies of the structure.

In this section, harmonic response of a composite plate is investigated. A composite plate is considered, which have a circular strip delamination around a circular hole delamination. Diameters of the circular hole delamination and the circular strip delamination are taken 20mm and 30mm, respectively.

A harmonic force is applied at the end of the cantilever-free composite plate and the frequency of the load is varying from 1Hz to 250Hz. Magnitude of the load is 1N and its phase angle is zero. Firstly, the natural frequencies are computed for the first there modes of the plate C with the modal analysis. Note that the first mode of the plate is the first bending mode and the third mode of that is the second bending mode. Table 8.7 lists the natural frequencies for the intact and delaminated clamped-free plates.

Table 8.7 Numerical results of the natural frequencies (Hz) for the clamped-free plates

	Intact Model	Circular Strip Delamination around Circular Hole Delamination
		Strip Delamination Dia. 30mm Hole Delamination Dia. 20mm
Mode	Plate 0	Plate C
1	34.293	34.152
2	111.33	110.65
3	215.30	211.39

Harmonic response of the node, which is the middle point of the free edge of the plate, is plotted in Figure 8.17. To get a better view of the harmonic response, scale of the vertical axis of the graph is selected logarithmic. From the results presented in this figure, it can be seen that the frequencies peaks approximately at 34 and 212Hz.

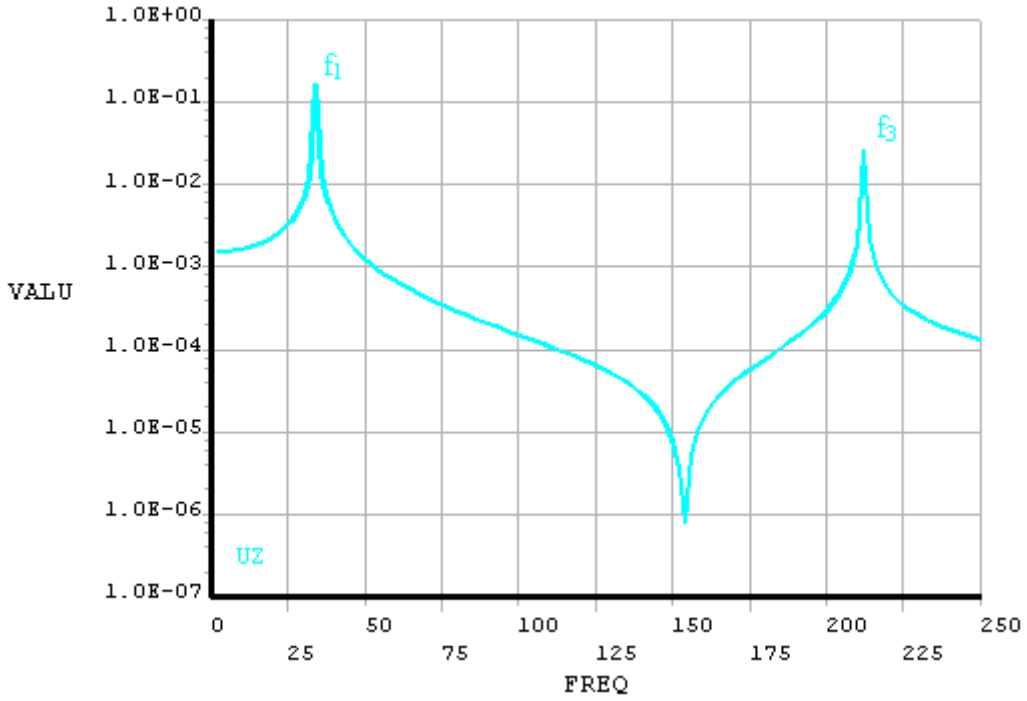

Figure 8.17 Harmonic response of the selected node

These correspond with the predicted frequencies of 34.152 and 211.39Hz. Also note that the natural frequency of the second mode of the plate does not seen in the Figure 8.17, cause of that mode is not a bending mode and the displacement of the selected node is insignificant at the load direction.

CHAPTER NINE

CONCLUSIONS

The delamination problem for laminated composite plates is analyzed in terms of some parameters such as the width and location of the delamination and types of boundary conditions using finite elements method and modal analysis. To achieve accurate results for delamination detection of laminated composite plate, a relatively fine mesh is considered for the finite element computation. The following conclusions may be drawn from the results of numerical simulation in this study.

- The natural frequency decreases in the existence of the delamination. The decreasing level depends on the size, location, and shape of the delamination. The decreasing level of the natural frequencies is also not the same for different modes.

- The natural frequency is significantly influenced by the delamination width. The natural frequency decreases with the increase of the delamination width due to the decrease in the stiffness.

- The natural frequency is significantly influenced by the delamination location with its width. The natural frequency increases as the delamination moves away along the axial direction from the clamped edge, and decreases as the delamination closes to twist point, and then increases again as the delamination moves away along the axial direction from the twist point of the plate. Changing level of the natural frequencies with the delamination location increases with the increase of the delamination width.

.

- Boundary conditions greatly affect the vibration characteristics of the plate. The natural frequency increases with the decrease of the degree of the freedom of the plate.

- The bending natural frequencies are minimum at different certain points for each bending mode and boundary conditions. This condition occurs due to the shape of the bending mode. These points are the elastic points of the plates.

- The first bending natural frequency of the clamped-free delaminated plate is close to that of intact one when the delamination is in the close vicinity of the free end of the clamped-free plate.

- The first bending natural frequency of the clamped-pinned delaminated plate is minimum where the delamination is at λ/l=0.65.

- The second bending natural frequency of the clamped-free delaminated plate is minimum where the delamination is at λ/l=0.60.

- The second bending natural frequency of the clamped-pinned delaminated plate is minimum where the delamination is at λ/l=0.80.

REFERENCES

Alnefaie, K. (2009). Finite element modeling of composite plates with internal delamination. *Composite Structures, 90*, 21-27.

Bathe, K. J. (1982) *Finite element procedures in engineering analysis*. New Jersey: Prentice-Hall.

Gadelrab, R. M. (1996). The effect of delamination on the natural frequencies of a laminated composite beam. *Journal of Sound and Vibration, 197(3),* 283-92.

Gören Kıral, B. (2009). Free Vibration Analysis of Delaminated Composite Beams, Science *and Engineering of Composite Materials, 16 (3),* 209-224.

Hua, N., Fukunagab, H., Kameyamab, M., Aramakib, Y., & Chang, F.K. (2002). Vibration analysis of delaminated composite beams and plates using a higher-order finite element. *International Journal of Mechanical Sciences, 44,* 1479-1503

Jones, R.M. (1975). *Mechanics of composite materials*. New York: McGraw-Hill Book Company.

Lee, J. (2000). Free vibration analysis of delaminated composite beams. *Composite Structures, 74(2),* 121-9.

Lin, D.X., Ni, R.G., &Adams, R.D. (1984) Prediction and measurement of the vibrational damping parameters of carbon glass fiber-reinforced plastics plates. *Journal of Computer Aided Materials Design, 18,* 132-52.

Ousset, Y., & Roudolff, F. (2000). Numerical analysis of delamination in multi-layered composite plates. *Journal of Computational Mechanics, 20,* 122-6

Qatu, M.S. (1991). Free vibration of laminated composite rectangular plates. *International Journal of Solids and Structures*, 941-54.

Qatu, M.S. (1994). Natural frequencies for cantilevered laminated composite triangular and trapezoidal plates. *Composites Science and Technology*, 441–9.

Qatu, M.S., & Leissa, A.W. (1991). Vibration studies for laminated composite cantilever plates. *International Journal of Mechanical Sciences*, 927-40.

Rikards, R. (1993). Finite element analysis of vibration and damping of laminated composites. *Composite Structures, 24,* 193-204.

Sankar, B.V. (1991). A finite element for modeling delaminations in composite beams. *Composite Structures, 38(2),* 239-46.

Wei, Z., Yam, L.H., & Cheng, L. (2004). Detection of internal delamination in multi-layer composites using wavelet packets combined with modal parameter analysis. *Composite Structures, 64,* 239-46.

Yam, L.H., Wei, Z., Cheng, L., & Wong, W.O. (2004). Numerical analysis of multi-layer composite plates with internal delamination. *Composite Structures, 82,* 627-37.

Zak, A., Krawczuk, M., & Ostachowicz, W. (2000). Numerical and experimental investigation of free vibration of multi-layer delaminated composite beams and plates. *Journal of Computational Mechanics, 26,* 309-15.